A high-efficiency high-power evanescently coupled UTC-photodiode[*]

Zhang Yunxiao(张云霄)[†], Liao Zaiyi(廖载宜), Zhao Lingjuan(赵玲娟), Zhu Hongliang(朱洪亮),
Pan Jiaoqing(潘教青), and Wang Wei(王圩)

(Key Laboratory of Semiconductor Materials Science, Institute of Semiconductors, Chinese Academy of Science, Beijing 100083, China)

Abstract: The effects of the multimode diluted waveguide on quantum efficiency and saturation behavior of the evanescently coupled uni-traveling carrier (UTC) photodiode structures are reported. Two kinds of evanescently coupled uni-traveling carrier photodiodes (EC-UTC-PD) were designed and characterized: one is a conventional EC-UTC-PD structure with a multimode diluted waveguide integrated with a UTC-PD; and the other is a compact EC-UTC-PD structure which fused the multimode diluted waveguide and the UTC-PD structure together. The effect of the absorption behavior of the photodiodes on the efficiency and saturation characteristics of the EC-UTC-PDs is analyzed using 3-D beam propagation method, and the results indicate that both the responsivity and saturation power of the compact EC-UTC-PD structures can be further improved by incorporating an optimized compact multimode diluted waveguide.

1. Introduction

High-speed photodetectors are key devices in the field of digital, as well as analogue, optical transmissions. In addition to their high bandwidth and high responsivity, there is a growing demand for large optical power handling capabilities of these devices. For instance, high-output photocurrent may trigger the decision circuits of digital receivers without the need for any electrical amplification. In analogue transmissions, the association of an externally modulated high-power and low-noise laser with a high power photodiode increases the dynamic range of the link. The unique feature of UTC-PD, which utilizes only electrons as the active carriers, is the key for its ability to achieve excellent high-speed and high-output characteristics simultaneously[1−4]. However, the tradeoff between quantum efficiency and transit time limits the responsivity for small devices that can operate at frequencies as high as 40 GHz. In recent years, evanescent edge coupled waveguide PDs have been applied widely because one can design independently PD structure (bandwidth) and fiber-device coupling (external quantum efficiency and high power handling capability), which allows for both high optical responsivity and high power[5−8]. Evanescently coupled photodiodes with an integrated taper have demonstrated a responsivity up to 0.75 A/W[9], but at the expense of a more complex (and thus, more difficult to fabricate) structure. The critical taper technology can be replaced by an etched short diluted multimode waveguide[10]. Using this approach, a responsivity of 1 A/W and saturation current of 11 mA have been demonstrated[11]. Efficiency and saturation power will be further improved by a new evanescently coupled uni-traveling-carrier photodiode

structure combining a multimode diluted waveguide structure with a uni-traveling-carrier photodiode structure. A novel evanescently coupled near-ballistic uni-traveling-carrier photodiode (EC-NB-UTC-PD) was reported and achieved extremely high responsivity (1.14 A/W) and a high saturation current (30 mA)[10]. Although high responsivity and high saturation power of the evanescently coupled uni-traveling-carrier photodiodes (EC-UTC-PDs) have been reported[12], the coupling process of the input optical signal to an EC-UTC-PD is too complicated to be theoretically analyzed. However, it is easier to investigate the coupling effect of the multimode diluted waveguide structures of the EC-UTC-PDs on quantum efficiency and power saturation through theoretical and experimental comparison.

In this paper, we design, fabricate, and test two evanescently coupled uni-traveling carrier photodiodes (EC-UTC-PD) with different multimode diluted waveguide (MDW) structures. Their respective performances regarding the multimode diluted waveguide design, efficiency and saturation current are analyzed and experimentally investigated.

2. Crystal growth and fabrication

The epitaxial structures of the developed EC-UTC-PDs are grown by MOCVD on a (100) S-doped InP substrate. Figures 1(a) and 1(b) show the schematic cross-sectional views of the demonstrated EC-UTC-PD1 and EC-UTC-PD2. The MDW consists of a diluted waveguide and the optical matching layers. The EC-UTC-PD1 is a conventional EC-UTC-PD structure with a multimode diluted waveguide integrated with
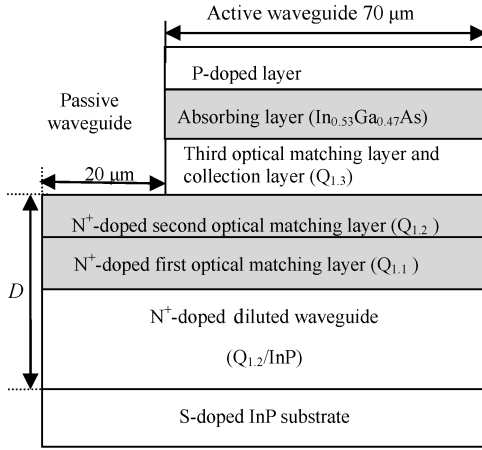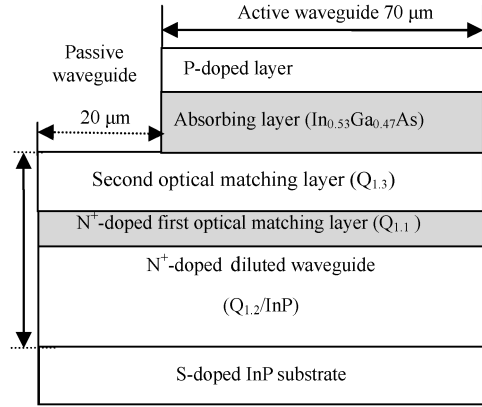
Fig. 1. Schematic cross-sectional views of the demonstrated EC-UTC-PDs: (a) EC-UTCPD1; (b) EC-UTC-PD2.

Table 1. Epi-structures of both EC-UTC-PDs.

Layer	Doping (cm^{-3})	EC-UTC-PD1	EC-UTC-PD2
$In_{0.53}Ga_{0.47}As$	P: 1×10^{19}	100 nm	
InP	P: 1×10^{18}	350 nm	
$In_{0.53}Ga_{0.47}As$	P: 1×10^{18}	250 nm	
$Q_{1.3}$	Undoped	300 nm	300 nm
	N: 1×10^{18}	0	100 nm
$Q_{1.2}$	N: 1×10^{18}	300 nm	0
$Q_{1.1}$	N: 1×10^{18}	250 nm	200 nm
$Q_{1.2}$ /InP	N: 1×10^{18}	80/300 nm	190/110 nm
		Four periods	Five periods
InP	N: 1×10^{18}	50 nm	
N-InP substrate			
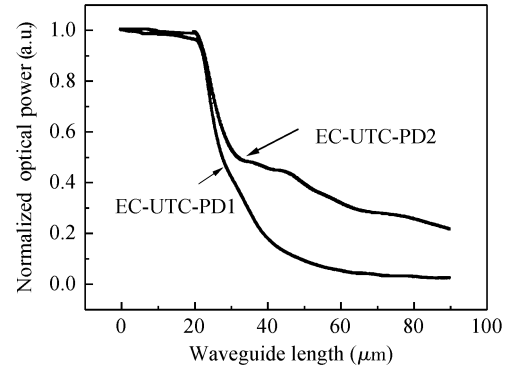
Fig. 2. Absorption curves of both EC-UTC-PDs.

a UTC-PD. The EC-UTC-PD2 is a compact one because the second matching layer of the multimode diluted waveguide is simultaneously used as collection layer of the UTC-PD as shown in Fig. 1. The epi-structures of the demonstrated EC-UTC-PDs were shown in Table 1. As seen in Table 1, the diluted waveguide of EC-UTC-PD1 adopted thin $Q_{1.2}$ ($Q_{1.2}$ denotes GaInAsP with bandgap wavelength $\lambda = 1.2 \ \mu m$) layers interspersed into the thick InP layers, which had a smaller effective reactive index, and that of the EC-UTC-PD2 utilizing thick $Q_{1.2}$ layers interposed into the thin InP layers has a larger effective reactive index. The total thickness D of the passive waveguide layers of the EC-UTC-PD2 and EC-UTC-PD2 were designed to be the same to eliminate the influence of the dimensions of input passive waveguide, and the respective thicknesses of the optical matching layers (shown in Table 1) were designed by three-dimensional (3-D) beam propagation method (BPM). The EC-UTC-PD epi-structures have been designed to have identical active layers thicknesses (0.25 μm-thick p- $In_{0.53}Ga_{0.47}As$ absorbing layer and 0.3 μm-thick undoped collection layer $Q_{1.3}$) and the photodiode structures have identical waveguide lengths (20 μm-long input passive waveguide and 70 μm-long active waveguide) for performance comparison. The input passive waveguide and the active waveguide have been designed to have the same width (5 μm), which makes the fabrication process easier. The two kinds of

EC-UTC-PD are fabricated by the same procedure as follows. First, the structure was etched over the full length of the photodiode and down to the N^+-doped InP layer with reactive ion etches (RIE) method, this layer is below the N^+-doped first optical matching layer followed by oxygen plasma cleaning and a sequence of wet etching to reduce the damage caused by RIE. Second, the active part of the waveguide was protected with silicon dioxide, and the remaining of the ridge of the waveguide was etched with a sequence of wet etching setups. Third, the whole waveguide was protected with silicon dioxide, and then removed the silicon dioxide on the top of the active waveguide. Finally, a Ti–Au deposition for p-contact, wafers were then lapped and polished down to about 70 μm and then the polished backside was covered with AuGeNi n-contact metallization. The samples were finally rapid-thermal annealed at 420 °C for 20 s to reduce contact resistance.

3. Optical simulation and experimental comparison

Three-dimensional (3-D) beam propagation method (BPM) software was used for optical simulation. This simulation was done by illuminating a light beam with a transverse electric (TE) mode into the MDW. Figure 2 shows the simulated absorption curves for both EC-UTC-PDs at 1550 nm wavelength. According to Fig. 2, about 82% of input optical power is gradually absorbed within 70 μm (from 20 to 90 μm
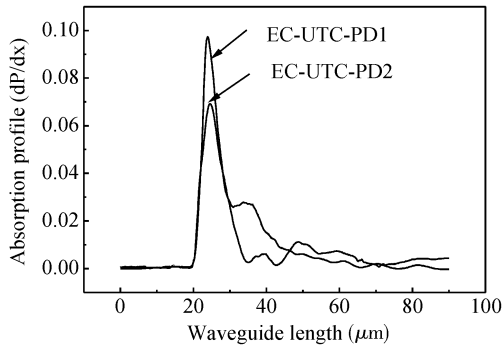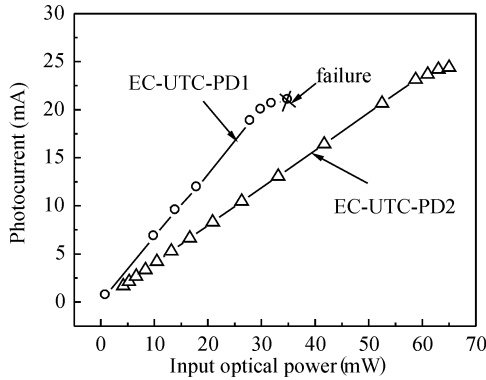
Fig. 3. Absorption profiles of both EC-UTC-PDs.

Fig. 4. Photocurrents of photodiodes as a function of input optical power at −2 V bias voltage.

shown in the plot) for the EC-UTC-PD1 and almost 67% of optical power is absorbed for the EC-UTC-PD2. The simulated effective indexes of MDWs for both EC-UTC-PD1 and EC-UTC-PD2 are very similar, therefore, the effect on efficiency and power saturation from reflection loss can be neglected. Assuming the internal quantum efficiencies are 100%, the corresponding responsivities of the EC-UTC-PD1 and the EC-UTC-PD2 are 0.73 and 0.55 A/W, respectively, without antireflection coating. The absorption in the EC-UTC-PD1 is more quickly, which shows that the multimode waveguide of the EC-UTC-PD1 was more efficient in driving the optical intensity from the passive waveguide to the active p-absorber than that of the EC-UTC-PD2. To investigate the saturation performances of these two photodetectors, their peak absorptions are simulated. The absorption profiles are shown in Fig. 3. As seen from Fig. 3, the peak absorption of the EC-UTC-PD2 occurs a little further away from the front end of p-absorber than that of the EC-UTC-PD1 and the peak absorption value of the EC-UTC-PD2 is about seven tenths of that of EC-UTC-PD1. In other words, the curve of the EC-UTC-PD1 is steeper than that of the EC-UTC-PD2. It clearly demonstrates that the peak absorption at the front end of the waveguide is more suppressed for the EC-UTC-PD2, which implies that the EC-UTC-PD2 can achieve higher saturation power.

We employed a tunable semiconductor laser as the light source for DC photocurrent measurement. The measured photocurrents of both EC-UTC-PDs as a function of the input optical power at a wavelength of 1550 nm under 2 V reverse bias are shown in Fig. 4. The measured responsivities of the

EC-UTC-PD1 and the EC-UTC-PD2 are 0.68 and 0.4 A/W, respectively. As expected, EC-UTC-PD1 shows a little higher responsivity compared with EC-UTC-PD2. The difference between the experimental values and the simulated ones could be result from the scattering loss in the passive waveguide and the imperfect internal quantum efficiency because some photons may waste their energy in free-carrier absorption and scattering loss during light propagation[13]. As seen from Fig. 4, the photocurrents of EC-UTC-PD1and EC-UTC-PD2 are linear up to input optical power of 30 and 59 mW respectively and then come to saturation. In addition, the cross in the figure shows the point where the EC-UTC-PD1 was destroyed, however, the breakdown of the EC-UTC-PD2 is not observed even at a high input power of 64 mW. Since the saturation level and the breakdown limit of EC-UTC-PD1 caused by electric field screening effect[14] should be the same as that of EC-UTC-PD2 (because they have the same UTC structure), the difference of the saturation behaviors was mainly due to the difference of the peak absorption between the EC-UTC-PD1 and the EC-UTC-PD2 and the failure of the EC-UTC-PD1 is thought to be due to the thermal effect[15, 16]. The experimental results show that the compacted EC-UTC-PD2 was much robust than the conventional EC-UTC-PD1 under high input power condition and verifies that the peak absorption in the active waveguide affects the saturation behavior.

Analytical and experimental results indicate that the responsivity and the saturation power of the modified EC-UTC-PD with a more compact waveguide design can be further improved by analyzing the absorption behavior using 3-D beam propagation method and optimizing the design of the multimode diluted waveguide structure. However, the optimum thicknesses of the multimode diluted waveguide layers can be different under different requirements. Based on the above analytical and experimental results, an optimized compact EC-UTC-PD structure was simulated by 3-D BPM software. Because the effective refractive index of the diluted waveguide in the EC-UTC-PD2 is too large to drive the input optical light into the absorption layer, the responsivity is suppressed. Therefore, the multimode diluted waveguide layers of the optimized compact EC-UTC-PD adopted four 0.08 μm-thick N$^+$-doped Q$_{1.2}$ layers alternating with five 0.3 μm-thick N$^+$-doped InP layers, and two optical matching layers (0.3 μm-thick N$^+$-doped Q$_{1.1}$ layer and 0.3 μm-thick undoped Q$_{1.3}$ layer). Figure 5 shows the calculated absorption curve and the absorption profile of the optimized EC-UTC-PD. As seen from Fig. 5(a), about 88% of input optical power is gradually absorbed within 70 μm (from 20 to 90 μm shown in the plot) for the optimized compact EC-UTC-PD. Assuming the internal quantum efficiencies are 100% and the input facet has an antireflection coating, the corresponding responsivities are 1.07 A/W. According to Fig. 5(b), two large absorption peaks of the EC-UTC-PD are observed. The first peak absorption is occurs at 7 μm away from the front end of p-absorber and its value is at least 2 times smaller than that of the EC-UTC-PD1. It clearly demonstrates that the peak absorption at the front end of p-absorber is highly suppressed and the total
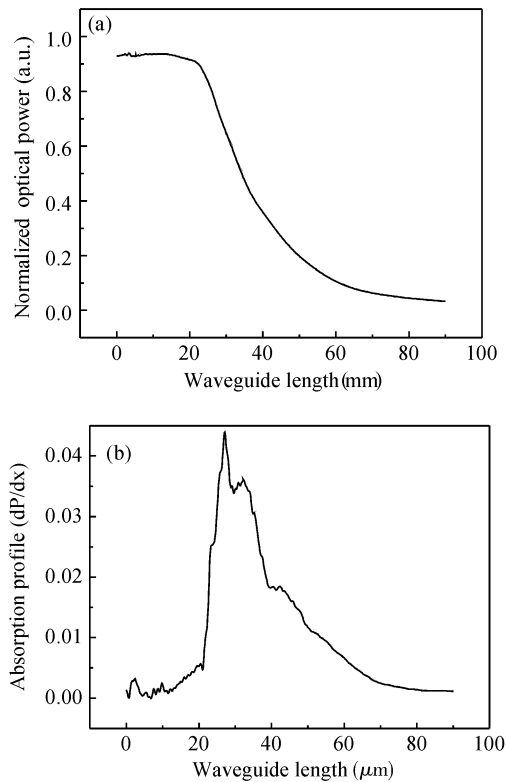
Fig. 5. (a) Absorption curves and (b) absorption profiles of the optimized compact EC-UTC-PD.

absorption efficiency is not reduced at the same time for this optimized compact EC-UTC-PD structure. Thus high responsivity and high saturation power of the compacted EC-UTC-PD can be achieved with a compact and optimized multimode diluted waveguide structure.

4. Conclusion

Effects of the multimode diluted waveguide of an evanescently coupled uni-traveling carrier photodiode structures on quantum efficiency and high power operations were investigated analytically and experimentally. A compacted EC-UTC-PD utilizes the second matching layer of the multimode diluted waveguide as collection layer of the UTC-PD, which can achieve high efficiency as well as saturation power. Further improvement in quantum efficiency and saturation characteristic is expected through optimization of the UTC-PD superstructure of the EC-UTC-PD and improvement in the quality of the photodiode epitaxial layers.

References

[1] Ishibashi T, Furuta T, Fushimi H, et al. InP/InGaAs uni-traveling-carrier photodiodes. IEICE Trans Electron, 2000, E83-C: 938

[2] Ishibashi T, Kodama S, Shimizu N, et al. High-speed response of uni-traveling carrier photodiodes. Jpn J Appl Phys, 1997, 36: 6263

[3] Ishibashi T, Furuta T, Fushimi H, et al. Photoresponse characteristics of uni-traveling-carrier photodiodes. Proc SPIE, 2001, 4283: 469

[4] Shimizu N, Watanabe N, Furuta T, et al. InP-InGaAs unitraveling-carrier photodiode with improved 3-dB bandwidth of over 150 GHz. IEEE Photonics Technol Lett, 1998, 10: 412

[5] Achouche M, Demiguel S, Derouin E, et al. New all 2-inch manufacturable high performance evanescent coupled waveguide photodiodes with etched mirrors for 40 Gb/s optical receivers. Proc Optical Fiber Communication Con., Atlanta, USA, 2003: 23

[6] Magnin V, Giraudet L, Harari J, et al. Design, optimization, and fabrication of side-illuminated p-i-n photodetectors with high responsivity and high alignment tolerance for 1.3- and 1.55-μm wavelength use. J Lightwave Technol, 2002, 20(3): 477

[7] Demiguel S, Giraudet L, Joulaud L, et al. Evanescently coupled photodiodes integrating a double-stage taper for 40-Gb/s applications–compared performance with side-illuminated photodiodes. J Lightwave Technol, 2002, 20(12): 2004

[8] Bach H G, Beling A, Mekonnen G, et al. InP-based waveguide-integrated photodetector with 100-GHz bandwidth. IEEE J Sel Top Quantum Electron, 2004, 10(4): 668

[9] Xia F, Thomson J K, Gokhale M R, et al. An asymmetric twin-waveguide high-bandwidth photodiode using a lateral taper coupler. IEEE Photonics Technol Lett, 2001, 13: 845

[10] Shi J W, Wu Y S, Wu C Y, et al. High-speed, high-responsivity, and high-power performance of near-ballistic uni-traveling-carrier photodiode at 1.55-μm wavelength. IEEE Photonics Technol Lett, 2005, 17(9): 1929

[11] Wu Y S, Shi J W, Chiu P H, et al. High-performance dual-step evanescently coupled uni-traveling-carrier photodiodes. IEEE Photonics Technol Lett, 2007, 19(20):1682

[12] Demiguel S, Li N, Li X, et al. Very high-responsivity evanescently coupled photodiodes integrating a short planar multimode waveguide for high-speed applications. IEEE Photonics Technol Lett, 2003, 15(12): 1761

[13] Fiedler F, Schlachetzki A. Optical parameters of In-based waveguides. Solid-State Electron, 1987, 30(1): 73

[14] Lin L Y, Wu M C, Itoch T, et al. High-power high-speed photodetectors—design, analysis, and experimental demonstration. IEEE Trans Microwave Theory Technol, 1997, 45: 1320

[15] Jasmin S, Vodjdani N, Renaud J, et al. Diluted-and distributed-absorption microwave waveguide photodiodes for high efficiency and high power. IEEE Trans Microwave Theory Tech, 1997, 45: 1337

[16] Harari J, Jin G, Vilcot J P, et al. Theoretical study of p-i-n photodetectors' power limitations from 2.5 to 60 GHz. IEEE Trans Microwave Theory Tech, 1997, 45: 1332